This article was downloaded by:
On: *25 January 2011*
Access details: *Access Details: Free Access*
Publisher *Taylor & Francis*
Informa Ltd Registered in England and Wales Registered Number: 1072954 Registered office: Mortimer House, 37-41 Mortimer Street, London W1T 3JH, UK

Separation Science and Technology
Publication details, including instructions for authors and subscription information:
http://www.informaworld.com/smpp/title~content=t713708471

Separation of Colloidal Particles from Nonaqueous Media by Cross-Flow Electrofiltration

Y. S. Lo[a]; D. Gidaspow[a]; D. T. Wasan[a]
[a] Department OF CHEMICAL ENGINEERING, ILLINOIS INSTITUTE OF TECHNOLOGY, CHICAGO, ILLINOIS

To cite this Article Lo, Y. S. , Gidaspow, D. and Wasan, D. T.(1983) 'Separation of Colloidal Particles from Nonaqueous Media by Cross-Flow Electrofiltration', Separation Science and Technology, 18: 12, 1323 — 1349
To link to this Article: DOI: 10.1080/01496398308059929
URL: http://dx.doi.org/10.1080/01496398308059929

PLEASE SCROLL DOWN FOR ARTICLE

Full terms and conditions of use: http://www.informaworld.com/terms-and-conditions-of-access.pdf

This article may be used for research, teaching and private study purposes. Any substantial or systematic reproduction, re-distribution, re-selling, loan or sub-licensing, systematic supply or distribution in any form to anyone is expressly forbidden.

The publisher does not give any warranty express or implied or make any representation that the contents will be complete or accurate or up to date. The accuracy of any instructions, formulae and drug doses should be independently verified with primary sources. The publisher shall not be liable for any loss, actions, claims, proceedings, demand or costs or damages whatsoever or howsoever caused arising directly or indirectly in connection with or arising out of the use of this material.

SEPARATION SCIENCE AND TECHNOLOGY, 18(12&13), pp. 1323-1349, 1983

Separation of Colloidal Particles from Nonaqueous Media by Cross-Flow Electrofiltration

Y. S. LO, D. GIDASPOW, AND D. T. WASAN

DEPARTMENT OF CHEMICAL ENGINEERING
ILLINOIS INSTITUTE OF TECHNOLOGY
CHICAGO, ILLINOIS 60616

Downloaded At: 13:32 25 January 2011

ABSTRACT

Charge characteristics of particles in aqueous or nonaqueous slurries are known to play an important role in solids-liquid separation processes. We have been conducting a fundamental study on filtration of colloidal particles suspended in nonaqueous media, such as coal and tar sand slurries based on their charge characteristics. This paper presents results of such a study involving cross-flow electrofiltration of nonaqueous slurries. Data are reported for α-$A\ell_2O_3$ particles suspended in tetralin. The effects of feed rate, driving pressure and electrical field strength on the filtration rate, total deposition rate on the central electrode, and the efficiency of the filter are presented.

The outlet slurry concentrations were measured with a specially built X-ray densitometer. These data are analyzed by a mathematical model using a Graetz-type analysis. The rate of deposition was found to be determined mainly by the electric field. The sludge flow near the central electrode significantly affected the efficiency of separation.

INTRODUCTION

A major problem in the development of coal liquefaction technology, and hydrocarbon production from tar sands and oil shale is the removal of colloidal particles. Charge characteristics of

Copyright © 1984 by Marcel Dekker, Inc. 0149-6395/84/1812-1323$3.50/0

particles in slurries are known to play an important role in solid-liquid separation processes (1-8). Electrokinetic phenomena which are induced by an externally applied field, may be utilized in an improved separation method.

Lee (9) showed how sedimentation of fine particles may be enhanced by the application of a high voltage electric field. A cross-flow electrofilter which utilized the electrophoretic motion of the particles to prevent filter clogging was invented by Gidaspow et al. (10). This work was described by Lee et al. (11) and continued by Liu (12). The cross-flow electrofilter was tested with a synthetic nonaqueous slurry as well as with samples of diluted H-coal process slurries. Liu et al. (13) developed a mathematical description of the corss-flow electrofilter by solving the Navier-Stokes equations for an annular flow with suction through an outer porous wall.

Downloaded At: 13:32 25 January 2011

The present work is a continuation of this nonaqueous solid-liquid separation study. The objective is to analyze the cross-flow electrofilter quantitatively. Extensive performance data, which included a measurement of the outlet slurry concentration by means of a specially constructed X-ray densitometer, were obtained. The deposition rate and the concentration distribution in the filter were examined theoretically using a Graetz-type analysis (14).

EXPERIMENTS

Cross-Flow Filter and an X-ray Densitometer

The cross-flow electrofiltration system, shown schematically in Figure 1, consisted of a feed tank, a slurry pump, a high volt-

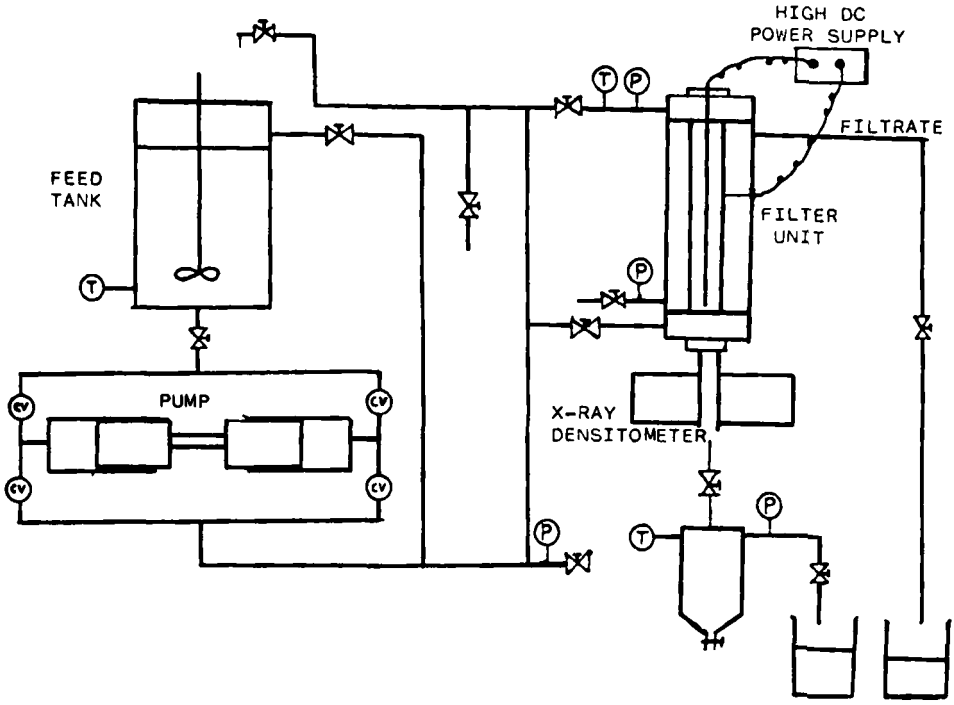

FIGURE 1. Schematic Block Diagram of Cross-flow Electrofilter

Downloaded At: 13:32 25 January 2011

age DC power supply, an electrofilter, and an X-ray densitometer system for measuring the concentration of the slurry.

The filter medium of the electrofilter is a porous stainless steel tube. The tube which was available with average pore diameters ranging from one to twenty microns, served as one of the electrodes. A platinum wire, which was installed to pass through the center of the filter served as the other electrode. The electrodes were housed in a steel tube, and were insulated from all other metal parts by Teflon. The slurry could be pumped through the porous tube and filled the annular space between the outer shell and the inner porous tube. A high enough electric field was

applied to cause the particles to move towards the platinum wire. The solids from the slurry deposited on the wire, while a clear boundary layer formed along the porous tube. Lee, et al..(11) give a more detailed description of the cross-flow fitter.

A Teflon tube with 0.2 cm thick wall was connected to the bottom of the filter. An X-ray density gauge measured the average density of either the feed or the slurry exiting the electrofilter. The densitometer consists of an 200 mCi Curium-244 source, a NaI crystal scintillation detector, an amplifier, a single channel analyzer, and a timer-counter.

Downloaded At: 13:32 25 January 2011

The curium source has a 17.8 years half-life. The principal emissions of the source are Pu L X-rays with photon energy between 12 and 23 Kev. At this energy level, the values of mass attenuation coefficients for tetralin and alumina particles are significantly different. For the present system, a maximum count rate of 40,000 counts/sec could be obtained. Other details of the experimental apparatus are discussed by Lo (15).

Experimental Conditions

A synthetic slurry made of tetralin and alumina particles was used in these experiments. A surfactant, Aerosol OT, sodium dioctyl sulfosuccinate, was used as a dispersant. The particles acquired a positive charge. The density gauge was calibrated to measure specific gravities of 0.960 to 0.980. In terms of a solid particle concentration, the range of measurement was 0.05 to 2.4 percent of solids by weight. The particle concentration of all feeds was 1.0 wt.%. The outlet concentrations were measured for

various feed rates and voltages. Experimental data were taken over a period of 30 minutes. The properties of the system are shown in Table 1.

The purpose of the first series of experiments was to find the deposition rate of particles onto the central electrode. In order to examine the effect of the electromotive force on particle deposition, no liquid was withdrawn from the shell side of the filter. Experiments were conducted for various feed rates and pressure drops across the filter tube with the field strength above the critical value needed to obtain a clear filtrate. In order to make sure that a clear boundary layer existed, a turbidimeter was used to measure the turbidity of the filtrate.

Downloaded At: 13:32 25 January 2011

Experimental Results and Discussions

Figure 2 shows the variation of a steady state outlet concentration with feed rate when there was no filtrate removed. The outlet concentrations were close to the inlet concentration for these runs with high feed rates or low applied voltages. The

TABLE 1.

Properties of α-$A\ell_2O_3$, Tetralin System

Inlet Solids Concentration:	1.0 wt.%
Average Particle Diameter:	0.3 μm
Density of the Slurry at 25°C:	0.971 gm/ml
Aerosol OT Concentration:	4.0 gm/liter
Electrophoretic Mobility:	0.05 μm/sec/V/cm
Bulk Conductivity of the Suspension:	1.4×10^{-8} mho/m
Viscosity of the Tetralin:	0.00224 Pa·Sec
Dielectric Constant of Tetralin:	2.7

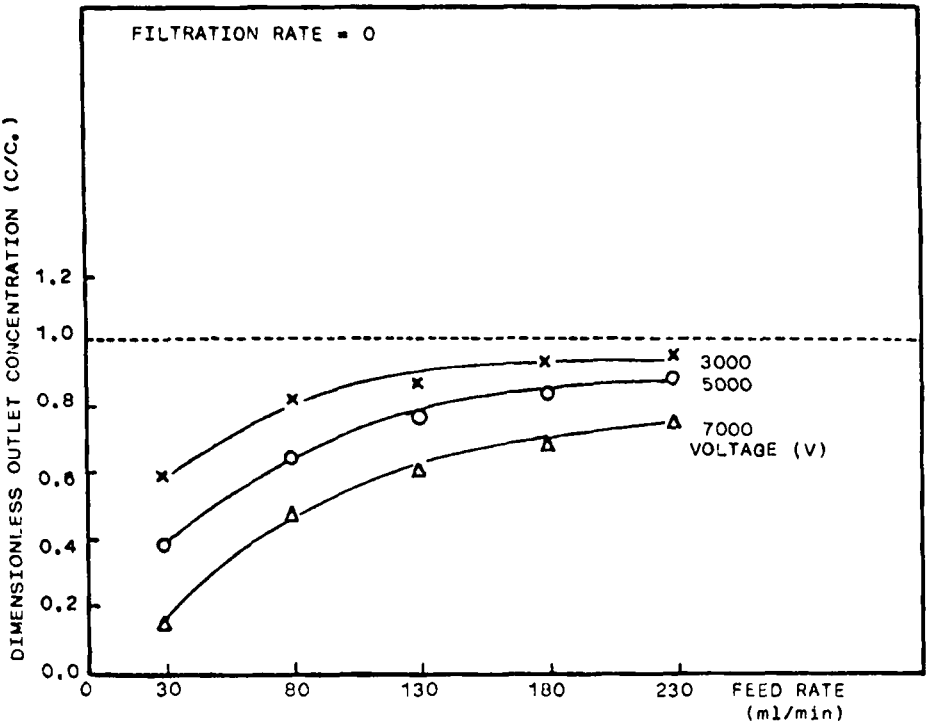

FIGURE 2. Dimensionless Outlet Concentration vs. Feed Rate

Downloaded At: 13:32 25 January 2011

dimensionless contact time defined in Figure 3 is proportional to the value of filter length (L) divided by the average velocity (Um). For zero contact time, the outlet concentration should be equal to the inlet concentration. The derivatives of these curves can be used to calculate the rate of deposition. This will be discussed later.

Figure 4 shows the efficiencies of the filter. They were calculated from the total weight of particles in the inlet and outlet streams. These data can also be used to obtain the total deposi-

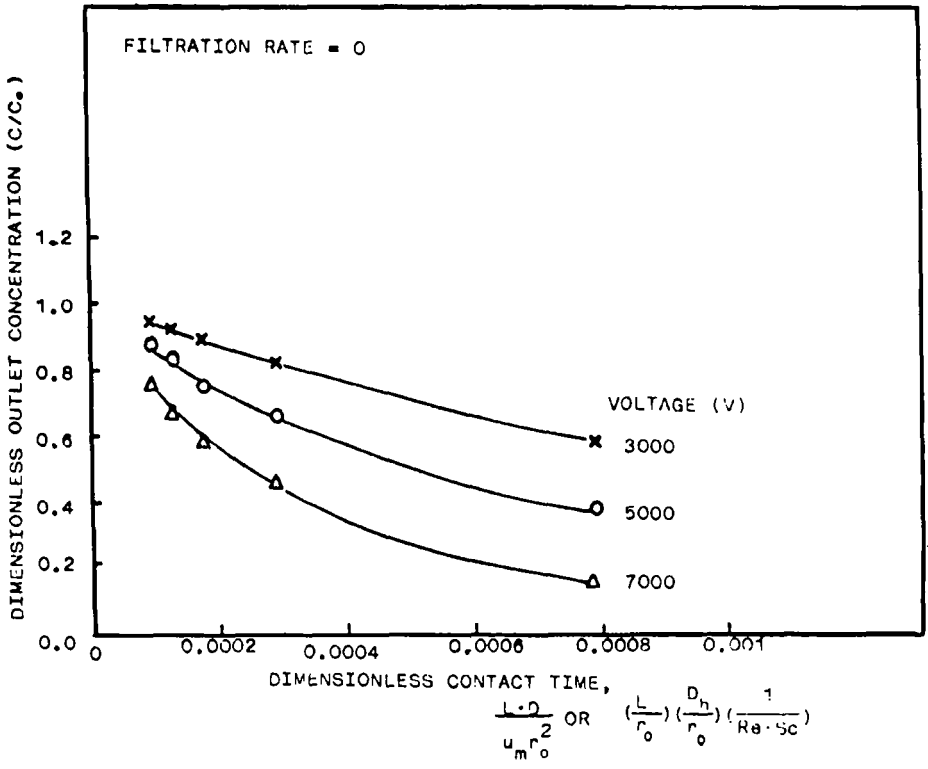

FIGURE 3. Dimensionless Outlet Concentration vs. Contact Time

tion rate by a material balance. Figures 5 and 6 show the effect of field strength and feed rate on the total deposition rate. The rates of deposition approach a constant when the feed rate is high.

Figure 7 shows the outlet concentration as a function of feed rate with various fractions of filtrate removed. These data show that as much as 70% of the feed can be removed as a clear liquid. The figure also shows that although this device is very efficient for producing a clear filtrate, it does not act as a good concen-

Downloaded At: 13:32 25 January 2011

Downloaded At: 13:32 25 January 2011

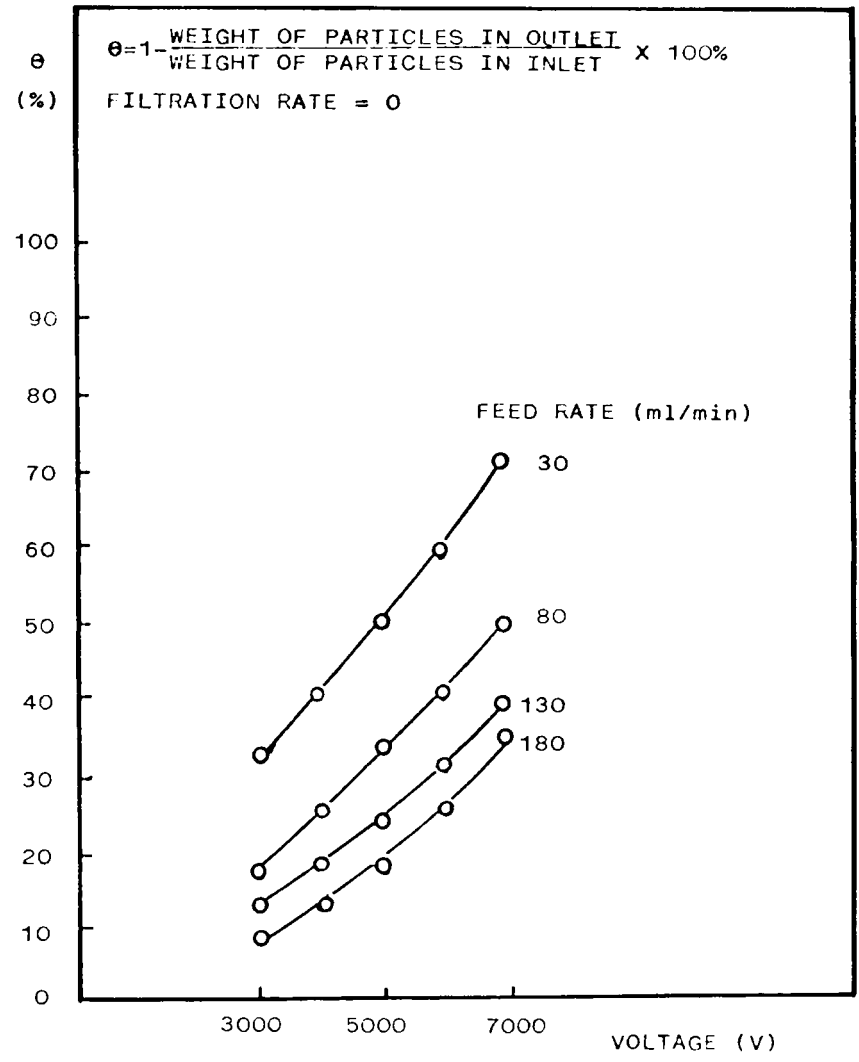

FIGURE 4. Efficiency of the Electrofilter

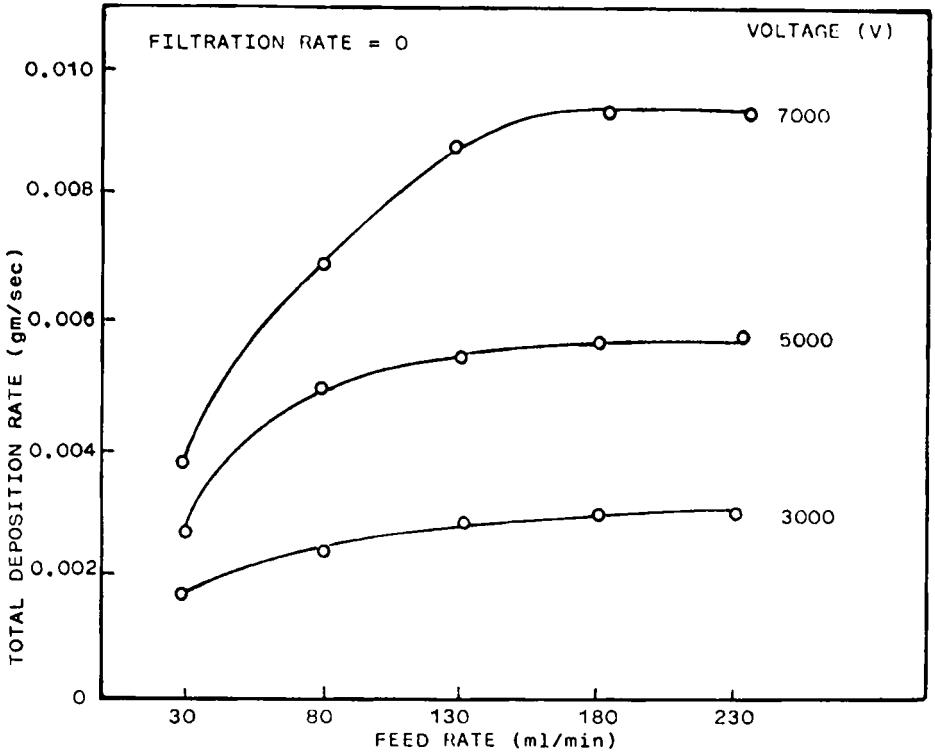

FIGURE 5. Total Deposition Rate vs. Feed Rate

trator of the feed. This suggests that the sludge layer be removed as a separate stream.

Experimental data for test times longer than 30 minutes indicated that the outlet concentration became unstable as the deposit on the wire grew and was sheared off. Therefore data for longer filtration runs are not presented.

THEORETICAL MODEL

As shown in the experimental study, a clear particle-free filtrate was obtained at voltages greater than the critical voltage.

Downloaded At: 13:32 25 January 2011

Downloaded At: 13:32 25 January 2011

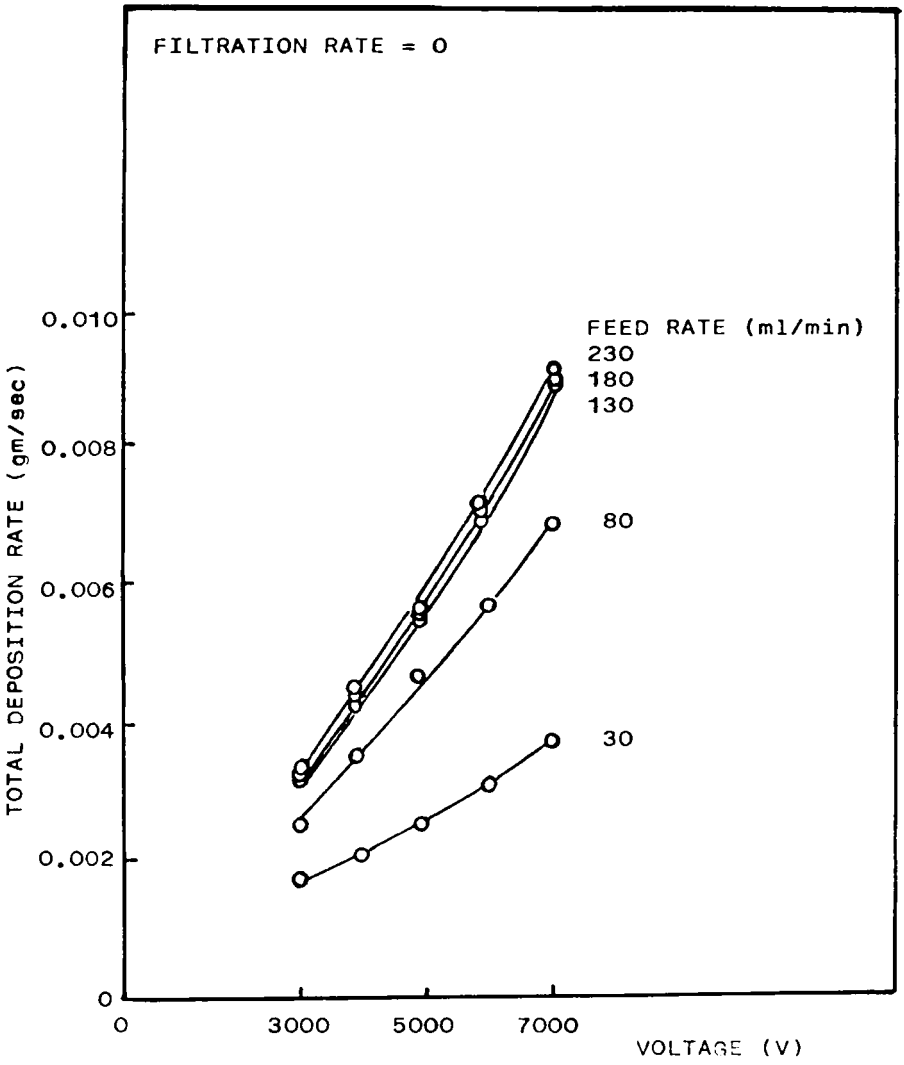

FIGURE 6. Total Deposition Rate vs. Field Strength

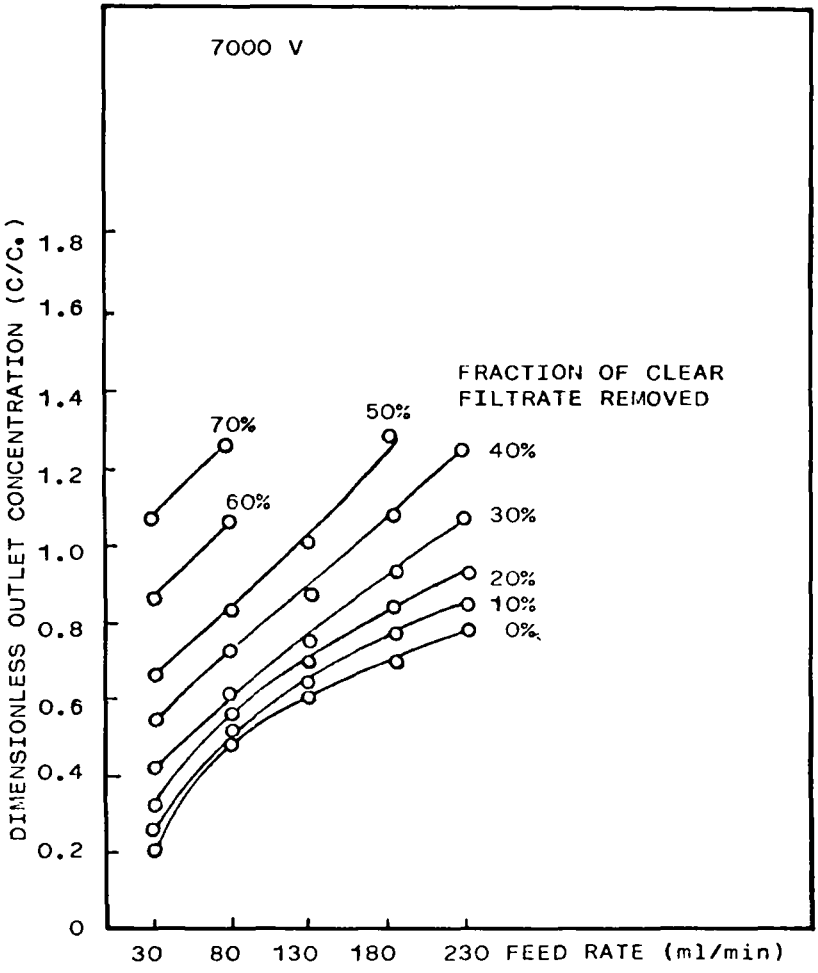

FIGURE 7. Dimensionless Outlet Concentration vs. Feed Rate

A clear boundary layer formation is expected to occur under these conditions. The objective of this theoretical study is to develop a mathematical model which describes the concentration distribution in the cross-flow electrofilter. The present work improved the previous models (11-13) by using a Graetz-type analysis, in which

Downloaded At: 13:32 25 January 2011

the local deposition rate is obtained by making suitable measurements of the mixing-cup concentration alone, without making any prior assumptions about the form of the rate function. Equations describing the sludge layer were also included in this model.

Figure 8 illustrates the geometry of the tubular cross-flow electrofilter. In cylindrical coordinates with the origin at the center of the cross section, x is taken in the direction of flow and r is the radial direction. The annular region is bounded by the two concentric tubes of radii r_i and r_o. u_m is the axial velocity at the inlet of the filter tube, and v_w is the withdrawal velocity at the filter wall. The electric field strength in an annulus from Gauss' law can be shown to be as follows.

$$E = \frac{V_a}{\ln (r_o/r_i)} \cdot \frac{1}{r} \tag{1}$$

where V_a is the applied voltage across the filter.

Downloaded At: 13:32 25 January 2011

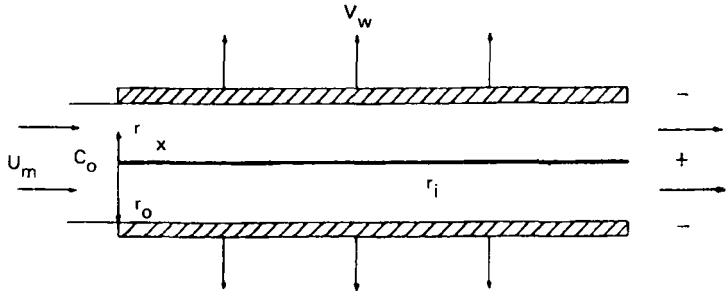

FIGURE 8. Tubular Cross-Flow Electrofilter

To develop a mathematical model describing the behavior of the filter, the following assumptions were made:

1. A steady state operation.
2. Uniform sludge layer on the central electrode as observed.
3. Fully developed velocity profiles outside the sludge layer.
4. Uniform withdrawal velocity at the porous wall.
5. Negligible longitudinal diffusion due to a high Peclet number.
6. Constant physical and transport properties.

As shown in Figure 9, r_s is the radius of the sludge layer, which can be measured experimentally. r_a is the local deposition rate on the sludge layer. Only a portion of those particles which

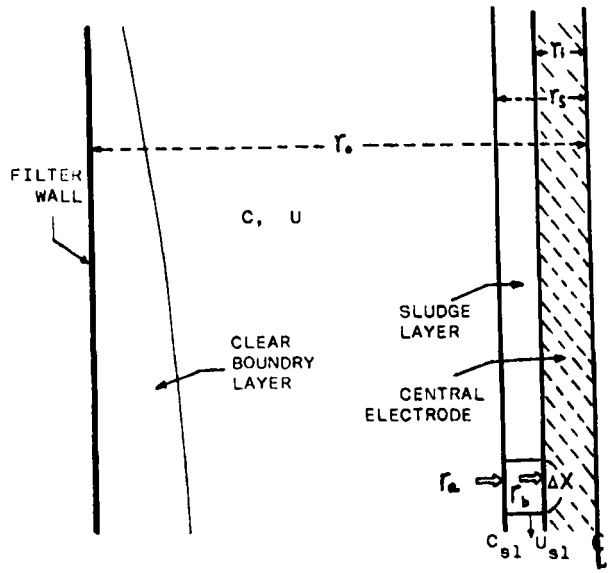

FIGURE 9. Material Balance of the Sludge Layer

Downloaded At: 13:32 25 January 2011

deposit on the sludge layer will actually deposit on the electrode with a rate of r_b. The other particles will be sheared off as the sludge flows with an average velocity, u_{sl} and concentration, c_{sl}. Therefore r_a can be related to r_b and u_{sl} by making the material balance:

$$r_a \cdot (2\pi r_s) = r_b \cdot (2\pi r_i) + \frac{d(c_{sl} \cdot u_{sl})}{dx} \cdot \pi (r_s^2 - r_i^2) \tag{2}$$

The mass balance on the particles outside the sludge layer results in the following partial differential equation

$$\frac{\partial (uc)}{\partial x} + \frac{1}{r} \frac{\partial}{\partial r} [r \cdot (v - EM \cdot E) \cdot c - D \cdot r \cdot \frac{\partial c}{\partial r}] = 0 \tag{3}$$

where u, v are the axial velocity and the transverse velocity, respectively (13), EM is the electrophoretic mobility, and D the diffusion coefficient.

$$B = \frac{k_s^2 - 1}{\ell n\, k_s} \qquad k_s = \frac{r_s}{r_o}$$

The boundary conditions for this system are

B.C. 1. Constant inlet concentration

$$c(0,r) = c_o \tag{4}$$

B.C. 2. Material balance on particles at the surface of central electrode

$$r_a = (EM \cdot E - v) \cdot c\Big|_{r=r_s} + D \frac{\partial c}{\partial r}\Big|_{r=r_s} \tag{5}$$

where the rate of deposition can be calculated from the experimental data.

B.C. 3. A leaky condition at the filter wall

Downloaded At: 13:32 25 January 2011

$$D\frac{\partial c}{\partial r}\Big|_{r=r_o} = v(1 - K)\cdot c\Big|_{r=r_o} - EM\cdot E\cdot C\Big|_{r=r_o} \qquad (6)$$

where the parameter K was defined as the ratio of particle velocity to bulk velocity by Liu et al. (13).

The governing equation and the boundary conditions were converted to dimensionless form using the following definitions:

$$C = \frac{c}{c_o} \qquad V = \frac{v}{v_w}$$

$$U = \frac{u}{u_m} \qquad X = \frac{L\cdot D}{u_m r_o^2} = \frac{L}{r_o}\cdot\frac{D_h}{r_o}\cdot\frac{1}{Re\cdot Sc}$$

$$\bar{r} = \frac{r}{r_o} \qquad Re = \frac{u_m\cdot\rho\cdot D_h}{\mu}$$

$$Sc = \frac{\mu}{\rho D} \qquad \alpha = \frac{r_o v_w}{D}$$

$$\beta = \frac{EM\cdot V_a}{D\cdot\ln(r_o/r_i)} \qquad k = \frac{r_i}{r_o}$$

$$R_a = r_a\cdot\frac{r_o}{Dc_o} \qquad k_s = \frac{r_s}{r_o}$$

$$R_b = r_b\cdot\frac{r_o}{Dc_o} \qquad P = \frac{c_{sl}\cdot u_{sl}}{c_o\cdot u_m}\cdot\frac{(k_s^2 - k^2)}{2k_s} \qquad (14)$$

Then the dimensionless equations are

$$R_a = R_b\cdot\frac{k}{k_s} + \frac{d\,P}{d\,X} \qquad (15)$$

and

$$\frac{\partial(UC)}{\partial X} + \frac{1}{\bar{r}}\cdot\frac{\partial}{\partial\bar{r}}\left[\alpha\bar{r}Vc - \beta C - \bar{r}\frac{\partial C}{\partial\bar{r}}\right] = 0 \qquad (16)$$

Downloaded At: 13:32 25 January 2011

The dimensionless boundary conditions become

$$\text{B.C. 1.} \quad C(0, \bar{r}) = 1 \tag{17}$$

$$\text{B.C. 2.} \quad \left.\frac{\partial C}{\partial \bar{r}}\right|_{\bar{r}=k_s} = \frac{-\beta}{k_s} \cdot C\Big|_{\bar{r}=k_s} + \alpha V C\Big|_{\bar{r}=k_s} + R_a \tag{18}$$

$$\text{B.C. 3.} \quad \left.\frac{\partial C}{\partial \bar{r}}\right|_{\bar{r}=1} = (1 - K) \cdot C\Big|_{\bar{r}=1} - \beta \cdot C\Big|_{\bar{r}=1} \tag{19}$$

Before this partial differential equation can be solved, the rate of deposition in the second boundary condition must be calculated.

Rate of Deposition

In order to isolate the effect of the transverse velocity in the filter tube, a flow through the filter with no filtrate withdrawal from the shell side is considered first.

Integration of equation (16) with respect to r from k_s to 1 yields

$$\frac{(1 - k_s^2)}{2} \cdot \frac{d C_m}{d X} + k_s \cdot R_a = 0 \tag{20}$$

and

$$R_a = - \frac{(1 - k_s^2)}{2k_s} \cdot \frac{d C_m}{d X} \tag{21}$$

where the mixing-cup concentration C_m is defined as

$$C_m = \frac{4}{(1-k_s^2)(1+k_s^2-B)} \int_{k_s}^{1} C(X,\bar{r})(1-\bar{r}^2+B \cdot \ell n\ \bar{r})\ \bar{r}\ d\bar{r} \tag{22}$$

This can be related to the dimensionless outlet concentration, C_E, which corresponds to the experimental measurement, and the sludge flow by making an overall material balance:

Downloaded At: 13:32 25 January 2011

$$C_E \cdot \pi(1 - k^2) = \int_{k_s}^{1} C(X,\bar{r}) \frac{2}{1+k_s^2-B} [1 - \bar{r}^2 + B \cdot \ell n\, \bar{r}] \cdot 2\pi\bar{r} \cdot d\bar{r}$$

$$+ \frac{c_{s1} \cdot u_{s1}}{c_o \cdot u_m} \pi(k_s^2 - k^2) \qquad (23)$$

Therefore

$$C_m = C_E - P \cdot \frac{2k_s}{(1-k^2)} \qquad (24)$$

or

$$\frac{d\,C_m}{d\,X} = \frac{d\,C_E}{d\,X} - \frac{d\,P}{d\,X} \cdot \frac{2k_s}{(1-k^2)} \qquad (25)$$

P is defined as

$$P = \frac{c_{s1}\, u_{s1}}{c_o\, u_m} \cdot \frac{(k_s^2 - k^2)}{2k_s} \qquad (26)$$

and is also related to the deposition rate R_a from equation (15):

$$\frac{d\,P}{d\,X} = R_a \cdot [1 - \frac{R_b \cdot k}{R_a \cdot k_s}] \qquad (27)$$

where $(R_b \cdot k)/(R_a \cdot k_s)$ is the ratio of particles which actually deposit on the electrode to those which deposit on the sludge layer. This ratio can be defined as a retention factor, F_r. The fraction of the particles which deposit on the sludge layer and are then sheared off to contribute to the outlet concentration is thus designated by $(1-F_r)$.

Although neither R_a nor R_b is known, their ratio can be obtained by comparing the outlet concentrations from the experimental

Downloaded At: 13:32 25 January 2011

data with those of two limiting cases. In the first case there is no deposition at all, although high voltages are applied. Hence, F_r equals zero and the outlet concentration as a function of filtration rate can be obtained from a material balance. The second limiting case is that flux of particles induced by the electric field is balanced by the rate of deposition. In this case all the deposited particles are retained on the electrode. Therefore R_a is the same as R_b and F_r equals 1. The actual behavior of the filter is between these two limiting cases. The retention factor can be defined as

$$F_r = \frac{R_b\, k}{R_a\, k_s} = \frac{C_1 - C_3}{C_1 - C_2} \tag{28}$$

where C_1, C_2, C_3 are the outlet concentrations of the first and second limiting cases, and the experimental measurement, respectively. Once F_r is known, equations (25) and (27) can be substituted into equation (21). Then

$$R_a = \frac{\dfrac{-(1 - k_s^2)}{2k_s}}{1 - \dfrac{(1 - k_s^2)}{(1 - k^2)} \cdot (1 - F_r)} \cdot \frac{d\, C_E}{d\, X} \tag{29}$$

Thus, equation (29) may be used to relate the deposition rate R_a to the measured outlet concentration C_E as a function of contact time, X.

Similarly, when there is a filtrate withdrawal from the filter, the deposition rate R_a can be obtained as follows:

Downloaded At: 13:32 25 January 2011

$$R_a = \frac{1}{1 - \frac{(1 - k_s^2)}{(1 - k^2)} \cdot (1 - F_r)} \cdot \left\{ \frac{\alpha}{k_s} \cdot C_E - \frac{(1 - k_s^2)}{2k_s} \left[1 - \frac{2\alpha X}{1 - k_s^2}\right] \frac{d\, C_E}{d\, X} \right\} \qquad (30)$$

Equation (29) is just a special case of equation (30) when α equals zero.

Equations (16) through (19) were solved numerically using a Crank-Nicholson finite difference method.

Results and Discussion

The calculated deposition rates as a function of contact time are shown in Figure 10. In this case, no filtrate was removed in

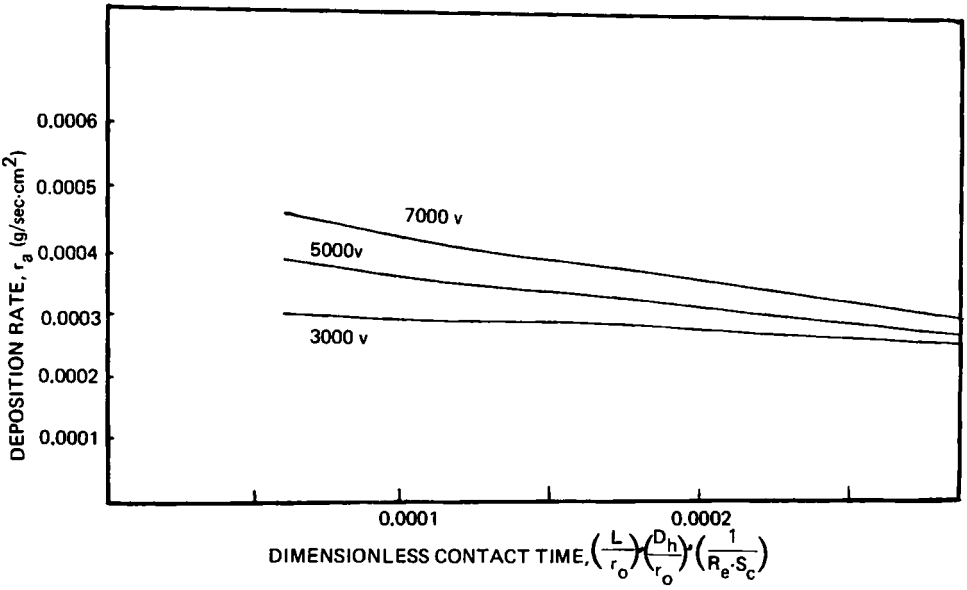

FIGURE 10. Deposition Rate vs. Dimensionless Contact Time

Downloaded At: 13:32 25 January 2011

order to obtain the deposition rate on the central electrode. As expected, the deposition rate increases with an increase in voltage and is maximum near the inlet.

The effect of the fraction of the clear filtrate removed on the mixing-cup concentration is shown in Figure 11. When the withdrawal velocity becomes higher, the concentration increases, but the thickness of the clear boundary layer decreases, as shown in Figure 12. The critical field strength, at which the clear boundary layer is just about to be formed, can be obtained, as shown in Figure 13. Figures 14 and 15 show that the maximum filtration rates for various field strengths can be obtained from the clear boundary layer thickness. Experimental data are lower than the

Downloaded At: 13:32 25 January 2011

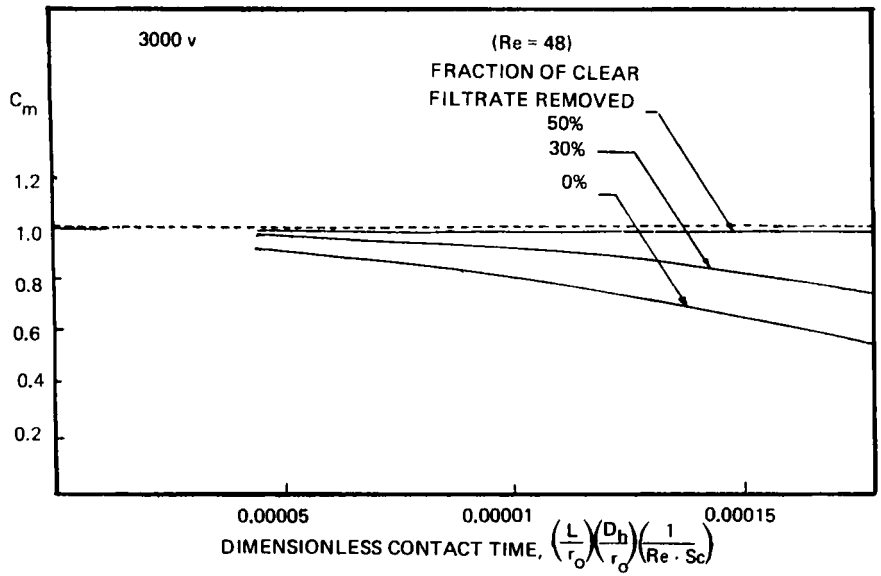

FIGURE 11. Effect of Filtration Velocity on the Mixing-cup Concentration

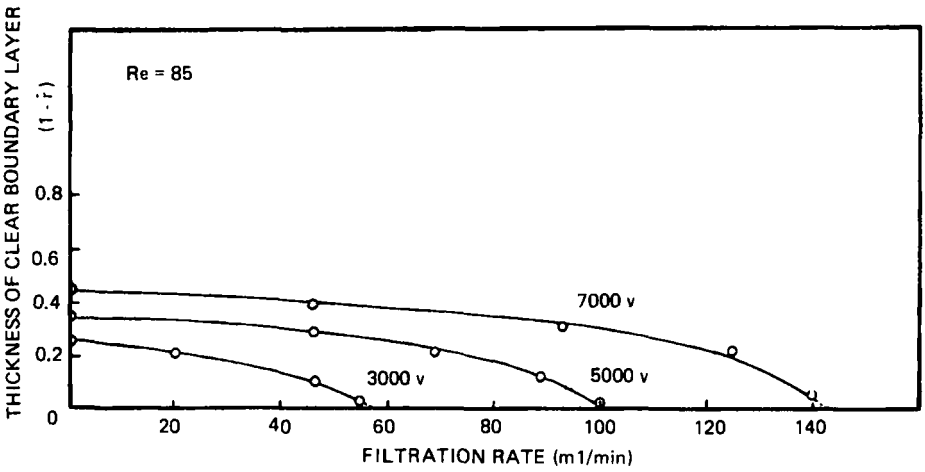

FIGURE 12. Effect of Filtration Velocity on the Clear Boundary Layer Thickness

Downloaded At: 13:32 25 January 2011

theoretical values, because it is difficult to operate under exactly critical conditions. It may also be caused by a distortion of the electric field due to the sludge layer, especially at high field strengths.

Figure 16 shows the flux as a function of the dimensionless contact time. The flux is expressed in terms of two driving forces namely the electric field and the concentration gradient as shown below.

$$\text{Flux} = EM \cdot E \cdot c_w - k_m(c_w - c_m) \qquad (31)$$

Where c_w is the estimated wall concentration from the experimentally determined outlet concentration, c_m, and k_m the mass transfer coefficient. Since in this system the value of the electric field

Downloaded At: 13:32 25 January 2011

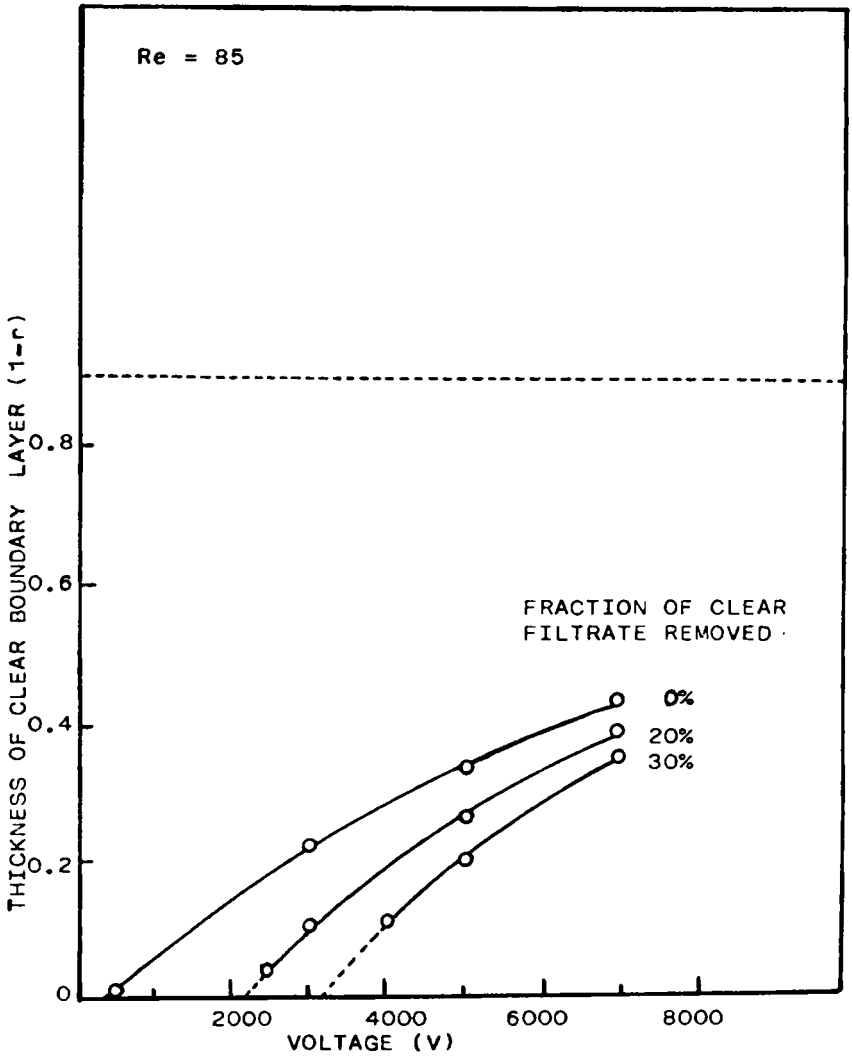

FIGURE 13. Effect of Field Strength on the Clear Boundary Layer Thickness for Three Different Filtration Velocities

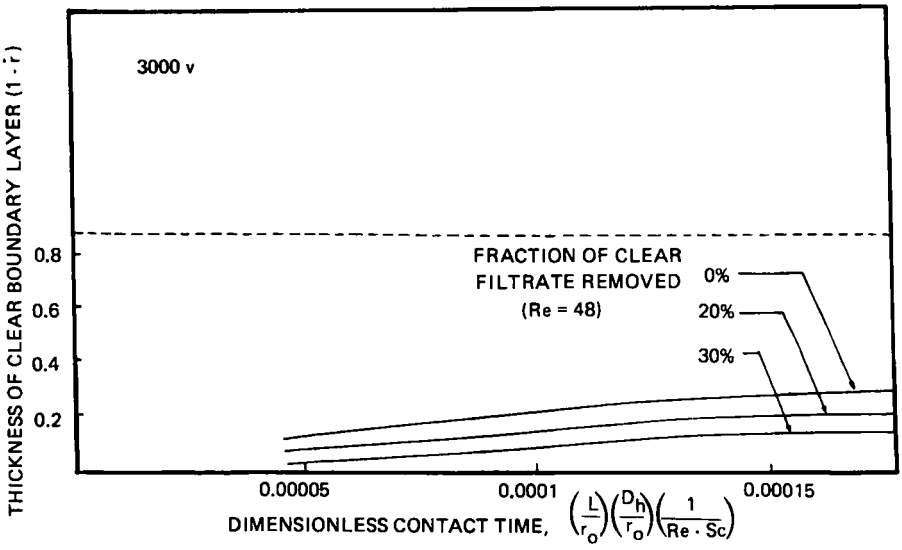

FIGURE 14. Thickness of Clear Boundary Layer vs. Filtration Rate

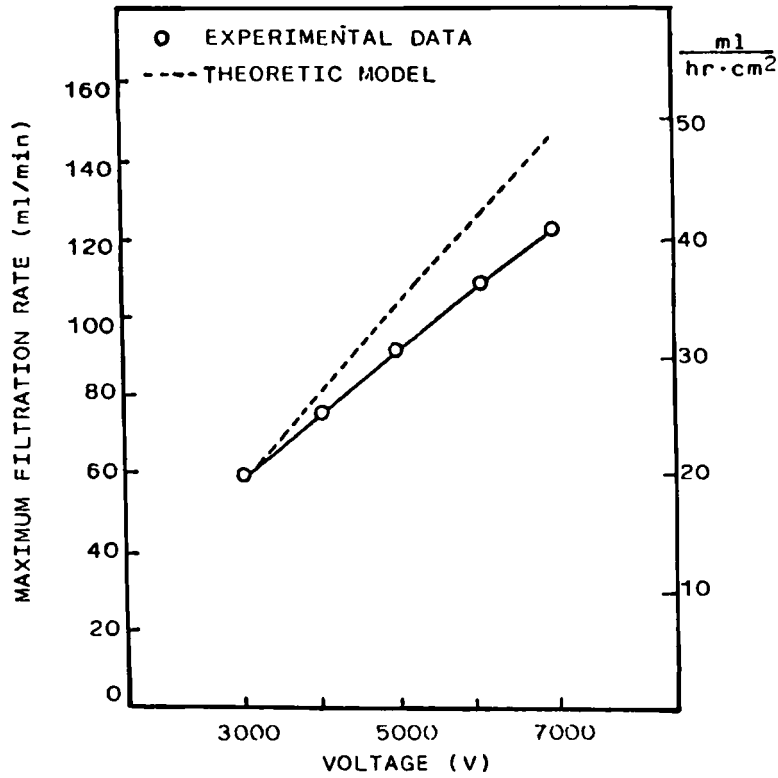

FIGURE 15. Effect of Field Strength on Maximum Filtration Rate

Downloaded At: 13:32 25 January 2011

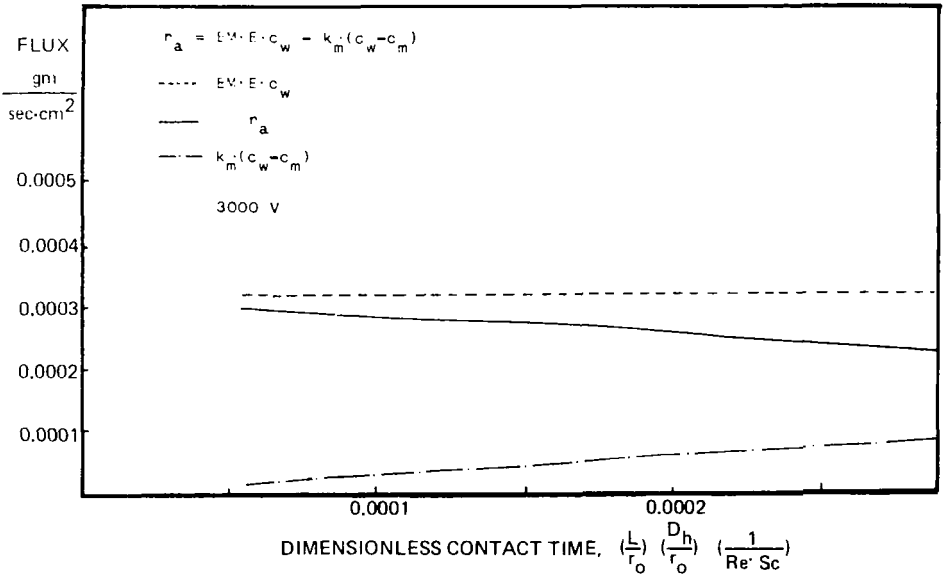

FIGURE 16. Flux on the Surface of Sludge Layer vs. Contact Time

is large, this figure shows that the greatest contribution to the flux is due to the imposed electric field. Figure 17 is a plot of the calculated mass transfer coefficient as a function of the voltage and the dimensionless contact time. As expected, the mass transfer coefficient is highest at the higher flow rate and is practically independent of the applied voltage.

Figure 18 shows a plot of the outlet concentration as a function of the Reynolds number in the electrofilter. It is evident that at very high velocities there is practically no sludge layer formation. However, at more practical conditions, the effect of the sludge layer becomes appreciable. Such data suggest again that the sludge layer should be separately removed.

Downloaded At: 13:32 25 January 2011

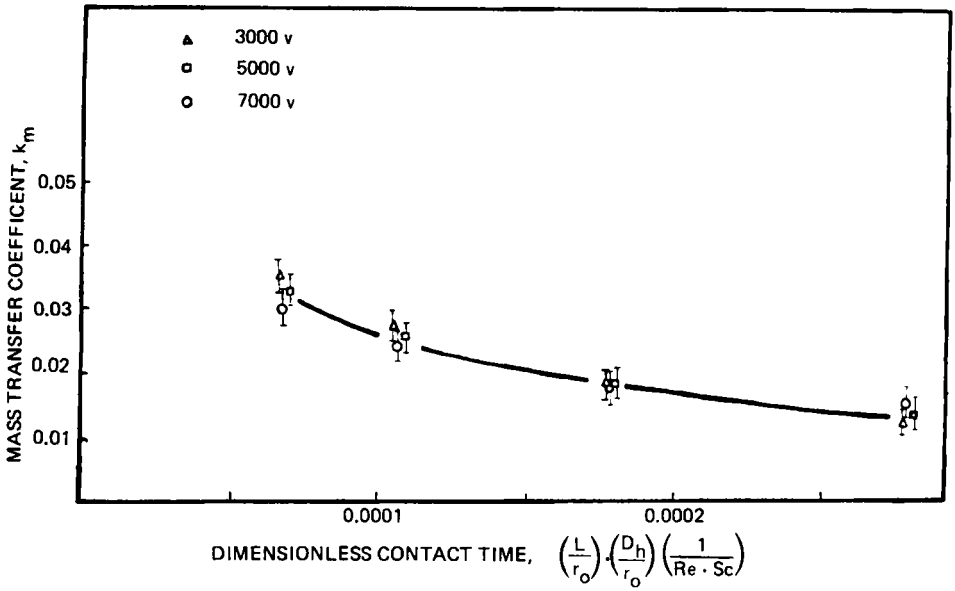

FIGURE 17. Mass Transfer Coefficient vs. Contact Time

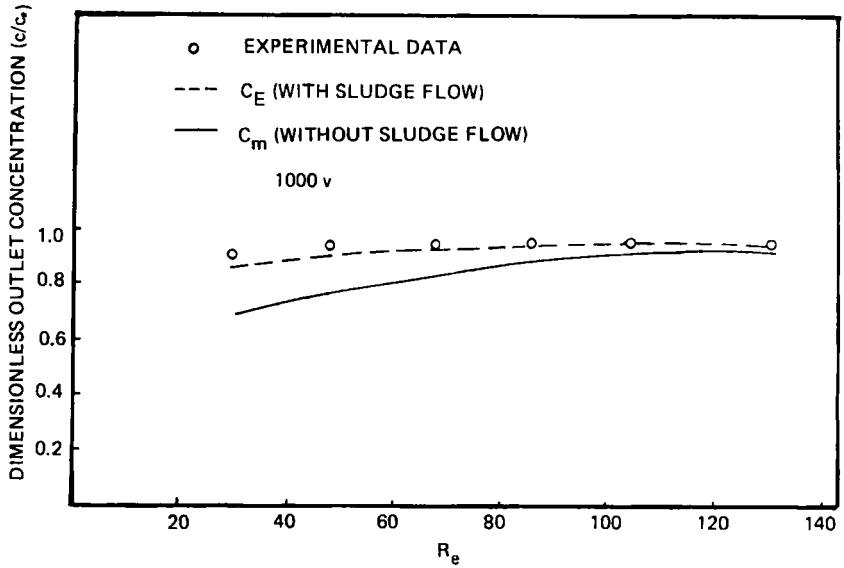

FIGURE 18. Comparison of the Calculated Mixing-cup Concentration with the Experimental Data

Downloaded At: 13:32 25 January 2011

Conclusions

1. The specially constructed X-ray densitometer made it possible to obtain accurate values of sludge concentrations as a function of contact time. These data were then used to obtain local deposition rates using a Graetz type analysis. Unfortunately the motion of the sludge layer greatly complicated the problem.
2. It was found that the main driving force for particle separation was the imposed high voltage electric field. As expected, the mass transfer coefficient was highest at highest flow rate and was practically independent of the applied voltage.
3. The retention factor, which represents the fraction of particle retained on the electrode is affected by the electric field strength and the Reynolds number. The data suggested the need for modifying the apparatus by withdrawing a sludge continuously to achieve an optimum separation of the slurry into a clear liquid and a highly concentrated sludge.

Downloaded At: 13:32 25 January 2011

ACKNOWLEDGEMENT

The financial support for this study was provided by the National Science Foundation Grants CPE-79-19189 and CPE 8218444.

REFERENCES

1. H. W. Chiang and C. Tien, Chem. Eng. Sci., 37, 1159, 1982.
2. R. Rajagopalan and T. E. Karis, AIChE Symposium Series, No. 190, 75, 72, 1979.

3. B. R. Rogers, Stability of Coal Derived Particles in Organic Media, Report No. ORNL-5631, Oak Ridge National Laboratories, Oak Ridge, TN (Aug. 1980).

4. M. P. Freeman, Chem. Eng. Prog. 78, 74, 1982.

5. D. E. Briggs, Paper presented at the Fine Particle Society Meeting, Maryland, 1980.

6. J. D. Henry Jr., L. F. Lawler and C. H. Alex Kuo, AIChE J., 23, 851, 1977.

7. S. P. Moulik, Env. Sci. and Tech., 5, 771, 1971.

8. R. J. Steininger, C. J. Radke and D. N. Hanson, Ind. Chem. Process Des. Dev., 18, 708, 1979.

9. C. H. Lee, Ph.D. Dissertation, Illinois Institute of Technology, Chicago, Illinois, 1978.

10. D. Gidaspow, C. H. Lee and D. T. Wasan, U.S. Patent 4,224,135 (1980) and U.S. Patent 4,248,686 (1981).

11. C. H. Lee, D. Gidaspow and D. T. Wasan, Ind. Eng. Chem. Fundamentals, 19, 166, 1980.

12. Y. Liu, Ph.D. Thesis, Illinois Institute of Technology, Chicago, Illinois, 1981.

13. Y. Liu, D. Gidaspow and D. T. Wasan, Particulate Sci. & Tech. J., 1, 27, 1983.

14. D. Gidaspow, AIChE J., 17, 19, 1971.

15. Y. S. Lo, Ph.D. Thesis, Illinois Institute of Technology, Chicago, Illinois, 1982.

Downloaded At: 13:32 25 January 2011